ResearchGate

See discussions, stats, and author profiles for this publication at: https://www.researchgate.net/publication/26768395

# Enhanced Uptake and Modified Distribution of Mercury(II) by Fulvic Acid on the Muscovite (001) Surface

**ARTICLE** *in* ENVIRONMENTAL SCIENCE AND TECHNOLOGY · AUGUST 2009

Impact Factor: 5.33 · DOI: 10.1021/es900214e · Source: PubMed

CITATIONS
25

READS
39

**4 AUTHORS**, INCLUDING:

Changyong Park
Carnegie Institution for Science
**100** PUBLICATIONS **1,191** CITATIONS

SEE PROFILE

Available from: Changyong Park
Retrieved on: 03 February 2016

# Enhanced Uptake and Modified Distribution of Mercury(II) by Fulvic Acid on the Muscovite (001) Surface

SANG SOO LEE,*,† KATHRYN L. NAGY,† CHANGYONG PARK,‡ AND PAUL FENTER‡

*Department of Earth and Environmental Sciences, 845 West Taylor Street MC-186, University of Illinois at Chicago, Chicago, Illinois 60607, and Chemical Sciences and Engineering Division, Argonne National Laboratory, 9700 South Cass Avenue, Argonne, Illinois 60439*

*Received January 21, 2009. Revised manuscript received May 8, 2009. Accepted May 18, 2009.*

Evidence is increasing for the mobility and bioavailability of aqueous mercury(II) species being related to the interactions of mercury with dissolved organic matter (DOM). Here, we assess the relative roles of the mineral surface and DOM in controlling mercury(II) uptake at the muscovite (001)−solution interface using interface-specific X-ray reflectivity combined with element-specific resonant anomalous X-ray reflectivity. Experiments were performed with single crystals of muscovite and solutions of 100 mg/kg Elliott Soil Fulvic Acid II and 0.5−1 × $10^{-3}$ mol/kg $Hg(NO_3)_2$ at pH 2−12. Mercury(II) adsorbed from a 1 × $10^{-3}$ mol/kg Hg(II) solution at pH 2 without fulvic acid (FA) as inner- and outer-sphere complexes that compensated 55(4)% of the permanent negative charge of the muscovite surface. The remaining charge presumably was compensated by hydronium. The enhanced uptake of Hg(II) (compensating 128% of the muscovite surface charge) and FA (43% more adsorbed compared to the amount from a similar solution without Hg), along with a broader distribution of Hg(II) at the interface, occurred by adsorption from a premixed solution of 1 × $10^{-3}$ mol/kg $Hg(NO_3)_2$ and 100 mg/kg FA at pH 2. Adsorption of Hg(II) and FA, likely as complexes, decreased significantly as pH increased from 3.7 to 12 in solutions of 0.5 × $10^{-3}$ mol/kg $Hg(NO_3)_2$ and 100 mg/kg FA. Preadsorbed FA molecules provide different binding environments and stability for Hg(II) than dissolved FA, which may be attributed to conformational differences, fractionation, or kinetic effects in the presence of the mineral surface, at least at these relatively high concentrations of aqueous Hg(II).

## Introduction

Mercury contaminates the environment from industrial and natural sources. These include the burning of fossil fuels, industrial incineration, and volcanism, all of which release Hg(0) or Hg(II) into the atmosphere, which is then returned to the surface by precipitation and dust deposition. Point sources from past agricultural practices, mining applications, or industrial spills release higher concentrations of mercury that spread locally in surface or ground waters. The concentration, and presumably transport, of Hg(II) in natural waters has been correlated with the dissolved organic matter (DOM) content (*1*−*3*). This association is an important but as yet poorly understood link in microbial methylation of Hg(II), the primary process by which mercury is taken up in the food chain (*4, 5*).

Natural organic matter (NOM) also exists as solid particulates in soils and sediments and often adheres to mineral surfaces via electrostatic and hydrophobic interactions. Whereas organic matter coatings can alter mineral reactivity (*6, 7*), the extent and reversibility of Hg(II) interactions with these coatings is less well-studied. We know, for example, from batch experiments, that fulvic acid (FA) complexation enhanced uptake of Hg(II) to the surface of goethite, especially at low pH (*8*), and that humic acid (HA)-coated kaolin minerals adsorbed more Hg(II) at pH 2.5−6.5 than those without HA (*9*). At the concentrations of these experiments, most Hg(II) interacts with the carboxylic or phenolic functional groups in organic matter, but the strongest binding is to the less abundant reduced sulfur groups, which dominate the association at the low mercury concentrations of many natural waters (*10*−*15*). Enhanced uptake in organic coatings on minerals should be influenced by the charge of the underlying surface in addition to the specific properties of the adsorbed organic molecules.

These competing influences on Hg(II) uptake can be visualized and quantified with molecular-scale resolution using in situ X-ray reflectivity (XR) methods (*16*−*19*), including resonant anomalous X-ray reflectivity (RAXR), which can selectively probe the distribution of a specific element at an interface (*20, 21*). Using specular XR, Lee et al. (*22, 23*) observed ∼1 nm thick FA films forming on the muscovite (001) surface in 100 mg/kg FA solutions at pH 3.7. However, the distribution of $Ba^{2+}$ added to this system could be inferred only by comparison to the system without FA and suggested direct adsorption to the underlying charged mineral surface, consistent with the weak affinity of $Ba^{2+}$ for organic ligands and hydration water.

Here, we have applied specular XR and RAXR together to assess the amount and distribution of FA and Hg(II) adsorbed onto the muscovite (001) surface. In terms of specific Hg(II) sorption processes, the results may be most relevant to severely contaminated sites where aqueous Hg(II) concentrations are similar to those applied for these experiments. More generally, the results show evidence at the angstrom scale for how the sorptive properties of FA change the uptake of organophilic metal cations on a negatively charged phyllosilicate mineral surface.

## Experimental Section

**Sample Preparation.** Solutions were prepared using Elliott Soil Fulvic Acid II (ESFA II) [International Humic Substances Society (IHSS), Section SI1 of the Supporting Information], high-purity $Hg(NO_3)_2 \cdot H_2O$, $HNO_3$, and NaOH. Concentrations of Hg(II) and FA were selected to maximize uptake and allow observation of distinctive changes at the interfaces. Dissolved concentrations of Hg(II) are expressed in units of mol/kg (molality, mol of Hg in 1 kg of water), whereas those of FA are in units of mg/kg (mg of dry FA in 1 kg of water). Compositions were 1 × $10^{-3}$ mol/kg $Hg(NO_3)_2$ at pH 2 (muHg2), 1 × $10^{-3}$ mol/kg $Hg(NO_3)_2$ and 100 mg/kg ESFA II at pH 2 (muHgFA2), and 0.5 × $10^{-3}$ mol/kg $Hg(NO_3)_2$ and 100 mg/kg ESFA II at pH 3.7, 5.5, 8.5, and 12 (muHgFA3.7, 5.5, 8.5, and 12, respectively). Mercury speciation was estimated with a thermodynamic model that included the major

* Corresponding author phone: (630)252-6679; fax: (630)252-9570; e-mail: sslee@anl.gov.
† University of Illinois at Chicago.
‡ Argonne National Laboratory.

10.1021/es900214e CCC: $40.75 © 2009 American Chemical Society
Published on Web 06/11/2009

functional groups in FA as ligands (Table S1 of the Supporting Information). Each experiment used a separate ASTM-V1 grade muscovite crystal (25.4 mm × 25.4 mm × 0.2 mm from Asheville Schoonmaker Mica Company) cleaved to expose a fresh (001) surface and reacted with solution in a 50 mL centrifuge tube wrapped with aluminum foil to prevent exposure to light. The muscovite was kept in a given solution for at least 2 h, which is long enough for dissolved FA to form a surface coating (*22, 23*). The wet crystal was then transferred to a thin-film sample cell (*18*) for reflectivity measurements.

One crystal was immersed in a 100 mg/kg ESFA II solution at pH 3.7 for 2 h after which an equal volume of $1 \times 10^{-3}$ mol/kg $Hg(NO_3)_2$ at pH 2.7 was added to test the effect of a presorbed FA film on Hg uptake (FAmuHg3). The crystal reacted with the final solution [$0.5 \times 10^{-3}$ mol/kg $Hg(NO_3)_2$ and 50 mg/kg ESFA II at pH 3] for five more hours.

**X-ray Measurements.** X-ray reflectivity (*R*, the ratio of the reflected to incident X-ray intensity) was measured in situ at a fixed photon energy (15−16.5 keV) as a function of momentum transfer (*q*) (Section SI2 of the Supporting Information) at beamline 11-ID-D of the Advanced Photon Source (APS), Argonne National Laboratory. All experimental systems had stable interfacial structures (i.e., <3% variation in reflectivity values measured at two momentum transfers near and away from Bragg reflections) except FAmuHg3, whose interfacial structure evolved during measurement (Figure S4b of the Supporting Information).

Reflectivity at the muscovite−solution interface shows typical large intensity variations with *q* (Figure 1a). The highest intensities occur in the tails of the bulk Bragg reflections and are mostly insensitive to the interfacial structure. Differences in interfacial structures, therefore, are most obvious in the reflectivity troughs (e.g., compare intensities highlighted in the vertical yellow bands in Figure 1a). The reflectivity data are also viewed in a normalized form $[R_{norm} = R[q\sin(qd/4)]^2$, where *d* is the (001) layer spacing] (*18*) to enhance the visibility of smaller but significant changes (Figure 1b). Element-specific RAXR spectra (i.e., reflectivity as a function of photon energy at fixed *q*) (Figure 2) were measured within ±0.4 keV of the $L_{III}$ absorption edge of Hg(II). The size and shape of the RAXR spectra depend on the distribution of interfacial Hg (Section SI3 of the Supporting Information). For example, the signal for muHgFA2 at $q = 0.22$ Å$^{-1}$, observed as a downward step in the reflectivity at the Hg−$L_{III}$ edge, is larger than those for the other experiments at a similar *q*, indicating a greater amount of sorbed Hg(II) (Figure 2). The rapid decrease in resonant amplitude with increasing *q* for muHgFA2 compared to that of muHg2 indicates that the distribution of Hg(II) is intrinsically broad and mercury ions may not be located at discrete sites.

**Data Analysis.** XR data were fit by parametrized structural models having three components: the ideal muscovite substrate lattice, the interfacial region including relaxed muscovite surface layers plus sorbed species, and the bulk water above the surface (Section SI4 and Table S2 of the Supporting Information). Sorbed FA was modeled as a layer composed of multiple overlapped Gaussian functions (*22, 23*) and identified as an extended range of electron density distinct from that for muscovite or bulk water in the derived total electron density profile. Quantitative characteristics of the FA layer are its thickness (Å) and laterally averaged electron density, including all sorbed species such as FA, Hg, and any $H_2O$ molecules (reported in dimensionless units of $\rho_{Weq}$, the electron density of the layer normalized to that of bulk water). RAXR data were fit by models of the distribution of interfacial Hg(II) (Section SI5 of the Supporting Information) as guided by an initial model-independent analysis (*24*). Parameters for all models were optimized using least-squares fitting procedures. For each experiment, the best-fit model was determined by the value of $\chi^2$, and the corresponding *R* factor is also reported.

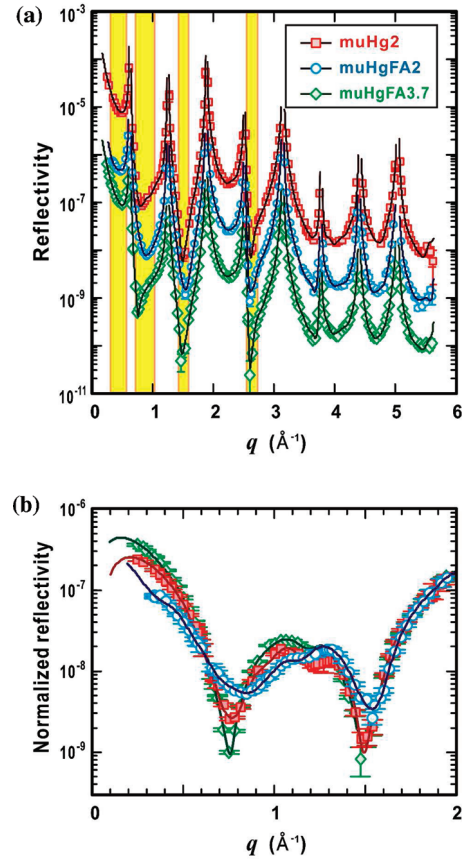


**FIGURE 1. (a) X-ray reflectivity for muscovite in a $1 \times 10^{-3}$ mol/kg $Hg(NO_3)_2$ solution in the absence and presence of 100 mg/kg ESFA II [muHg2 (red □ scaled by a factor of 10) and muHgFA2 (blue ○), respectively] at pH 2 compared to that in a solution of $0.5 \times 10^{-3}$ mol/kg $Hg(NO_3)_2$ and 100 mg/kg ESFA II at pH 3.7 [muHgFA3.7 (green ◇ scaled by a factor of $10^{-1}$)]. Lines through the data points are calculated reflectivities from the best-fit models. Yellow bands highlight *q* ranges showing clear differences in data among experiments. (b) Normalized reflectivity is shown over a selected range of *q* to emphasize the significant (~5-fold) differences in reflectivity. The same symbols are used for the data sets in panel a but without vertical scaling.**

## Results and Discussion

Here, we demonstrate how FA affects the uptake of Hg(II) at the muscovite surface by first showing results for $Hg^{2+}$ adsorption in the absence of FA at pH 2 and then comparing sorption from mixed Hg(II)−FA solutions with sorption of FA alone at the same pH. From there, it is straightforward to assess the effect of pH on Hg(II) adsorption from mixed Hg(II)−FA solutions and the influence of a pre-existing FA film.

**Sorption of $Hg^{2+}$ on Muscovite at pH 2.** The total electron density profile derived from the XR data for muHg2 shows one broad peak 2.54(11) Å (1$\sigma$ uncertainties of the estimated fitting parameters are in parentheses and apply to the last digit or digits) above the muscovite surface (Figure 3a). This shape is distinct from the two sharp near-surface peaks observed at the muscovite−water interface (muDIW5.5 in Figure 3a) (*17*), suggesting that adsorbed $Hg^{2+}$ perturbs the surface hydration structure. Analysis of the RAXR data shows that $Hg^{2+}$ occurred at two heights [0.62(5) and 3.58(4) Å] with a smaller fraction distributed farther away in a broad peak

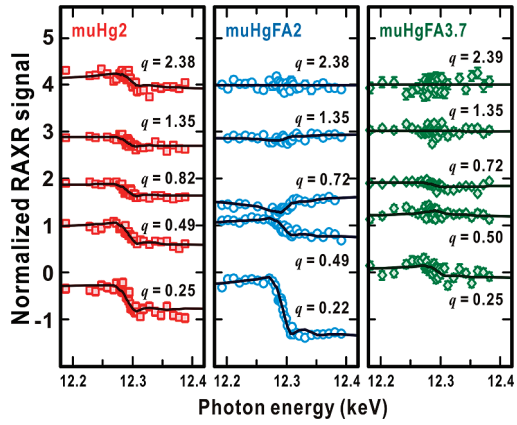


**FIGURE 2. Normalized RAXR signal using the resonance amplitude normalization $[(|F_{tot}(q,E)|^2 - |F_{NR}(q)|^2)/(2|F_{NR}(q)|)$, where $F_{tot}$ and $F_{NR}$ are total and nonresonant structure factors, respectively (Section SI5 of the Supporting Information)] at the selected $q$ (Å$^{-1}$) for muscovite in solutions of 1 × 10$^{-3}$ mol/kg $Hg(NO_3)_2$ at pH 2 (muHg2), 1 × 10$^{-3}$ mol/kg $Hg(NO_3)_2$ and 100 mg/kg ESFA II at pH 2 (muHgFA2), and 0.5 × 10$^{-3}$ mol/kg $Hg(NO_3)_2$ and 100 mg/kg ESFA II at pH 3.7 (muHgFA3.7). Each data set is shifted vertically by 1 unit for visual comparison.**

centered at 9.57(38) Å. The total coverage of 0.26(2) Hg per unit cell area ($A_{UC}$) compensates 55(4)% of the layer charge (0.966 $e^-/A_{UC}$) (*22*) of the muscovite surface (Table 1). The remaining negative charge is likely compensated by hydronium, which is 10 times more concentrated than $Hg^{2+}$ in solution.

The first peak at 0.62(5) Å corresponds to the calculated position of $Hg^{2+}$ above a ditrigonal cavity, 0.68 Å, assuming close-packing of bare $Hg^{2+}$ (ionic radius of about 1 Å) with three inner-oxygen atoms of a ditrigonal cavity that form a triangle having sides ~4 Å long: this species is interpreted as an inner-sphere (IS) complex. The second peak is more distant than any possible IS Hg species and corresponds to the height of an outer-sphere (OS) complex, which is most likely $Hg(H_2O)_6^{2+}$ (*25*) (Figure 4). The breadth of the second peak indicates that OS $Hg^{2+}$ may be more mobile than the IS species or perhaps present at multiple heights (see other sorption models in Section SI6 of the Supporting Information) that were indistinguishable within experimental resolution (~1 Å). The third broad peak extending from 6 to 13 Å above the surface indicates an additional distribution of OS Hg(II). The full width at half-maximum of this peak [5.3(13) Å] is much narrower than the Debye length (34 Å) of $Hg^{2+}$ predicted by the linearized Poisson−Boltzmann electrical double-layer model (*26*). This comparison shows that the distribution of Hg(II) in the third peak cannot be described simply by a classical diffuse ion profile. Some of the OS Hg(II) may maintain higher order hydration shells and/or adsorb onto the hydrated muscovite surface.

The dominantly bimodal distribution of $Hg^{2+}$ at pH 2 on the muscovite basal surface is similar to that of adsorbed $Sr^{2+}$ observed with RAXR in 1 × 10$^{-2}$ M $Sr(NO_3)_2$ at pH 5.5 (*20*). However, in montmorillonite and vermiculite clay interlayers, Hg is coordinated either as a fully hydrated species or in a mercuric oxide structure based on interpreted extended X-ray absorption fine structure (EXAFS) spectra (*27*). Adsorption is driven by electrostatic interactions on the (001) surfaces of these layer silicates, and the prevalence of IS $Hg^{2+}$ on muscovite might be explained partly by the larger amount of permanent structural charge in its basal tetrahedral sheet. This is consistent with recent observations of a change in $Sr^{2+}$ adsorption from mixed IS/OS species to a single OS species, when there is an apparent reduction of the surface charge of the muscovite by hydronium adsorption (*21*).

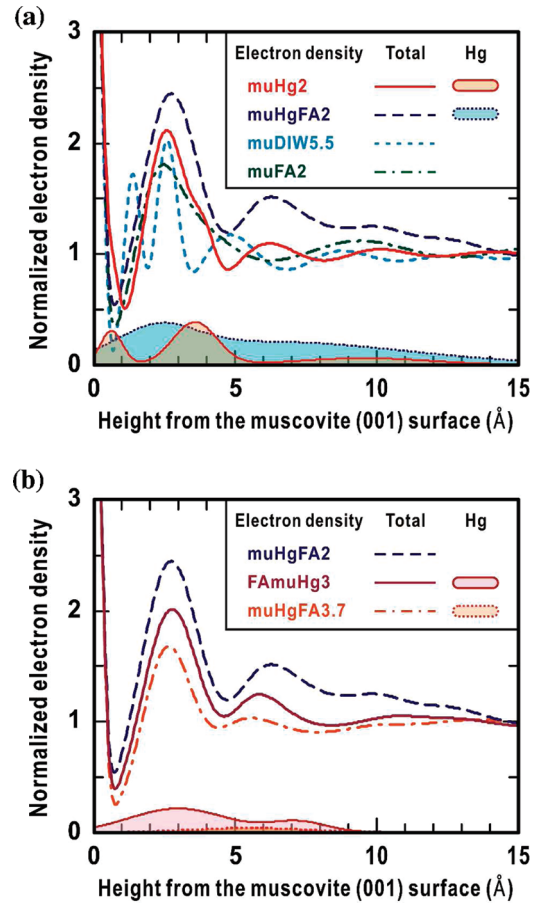


**FIGURE 3. Electron density profiles for the best-fit models of the interfacial structure for muscovite reacted (a) in 1 × 10$^{-3}$ mol/kg $Hg(NO_3)_2$ at pH 2 (muHg2, solid red line) and a 1 × 10$^{-3}$ mol/kg $Hg(NO_3)_2$ and 100 mg/kg ESFA II solution at pH 2 (muHgFA2, long-dashed blue line) compared to deionized water at pH 5.5 (muDIW5.5, short-dashed sky blue line) (*17*) and a 100 mg/kg ESFA II solution at pH 2 (muFA2; dotted-dashed green line) (*23*) and (b) in a pH 3.7 ESFA II solution (100 mg/kg) to which an equal volume of pH 2.7 $Hg(NO_3)_2$ solution (1 × 10$^{-3}$ mol/kg) was added producing a final pH near 3 (FAmuHg3, solid purple line) compared to muHgFA2 (long-dashed blue line) and muHgFA3.7 (0.5 × 10$^{-3}$ mol/kg $Hg(NO_3)_2$ and 100 mg/kg ESFA II solution at pH 3.7, dotted-dashed orange line). Electron density profiles of interfacial Hg derived from the best-fit models of RAXR are shown as shaded areas. Electron density was normalized to that of bulk water and is not shown below 0 Å.**

**Enhanced Sorption of Mercury(II) and Fulvic Acid on Muscovite at pH 2.** When a muscovite crystal reacted with a Hg(II)−FA solution at pH 2 (muHgFA2), the organic film containing both Hg(II) and FA was more electron dense than that previously observed for sorbed FA alone (muFA2) (*23*). The total electron density profile for the Hg(II)−FA film has one broad near-surface peak, a second less intense peak, and a gradually tapering tail (Figure 3a) with an average electron density of 1.34 $\rho_{Weq}$, which is higher than 1.13 $\rho_{Weq}$ for the FA film without Hg (*23*). Mercury(II)-specific distribution is broad, continuous, and lacking in sharp individual peaks. The total coverage of 0.62(5) atom/$A_{UC}$ is 140% higher than that without FA (muHg2) (Table 1), indicating that the sorbed species may be Hg(II)−FA complexes formed in the initial mixed solution. The total coverage may effectively compensate 128(10)% of the surface layer charge of the muscovite; however, exact mechanisms of charge compensation are unknown. Excess Hg(II) could bind mainly to functional groups in the sorbed FA and some may possibly bridge FA to the muscovite surface.

**TABLE 1. Characteristics of Hg and FA Adsorbed onto the Muscovite Surface[a]**

| | | interfacial Hg peak | | | FA layer | |
|---|---|---|---|---|---|---|
| sample[b] | $\chi^2$ (R factor)[c] | position (Å) | occupancy (atom/$A_{UC}$) | distribution width (Å) | thickness (Å) | average layer density ($\rho_{Weq}$)[d] |
| muHg2 | 1.15(0.005) | 0.62(5) | 0.06(1) | 0.13(f) | | |
| | | 3.58(4) | 0.14(1) | 0.68(6) | | |
| | | 9.57(36) | 0.06(2) | 2.26(55) | | |
| muHgFA2 | 1.22(0.004) | 2.28(7) | 0.15(2) | 1.28(11) | 14.9 | 1.34 |
| | | 6.28(27) | 0.47(5) | 4.71(25) | | |
| FAmuHg3 | 1.48(0.005) | 2.98(14) | 0.18(2) | 1.63(17) | 7.7 | 1.24 |
| | | 7.22(27) | 0.05(1) | 0.90(26) | | |
| muHgFA3.7 | 1.07(0.006) | 5.53(22) | 0.04(1) | 1.88(40) | 7.2 | 1.05 |
| muHgFA5.5 | 1.17(0.007) | 5.34(31) | 0.02(1) | 0.93(50) | 6.7 | 1.10 |
| muHgFA8.5 | 2.33(0.053) | 2.47(39) | 0.05(1) | 1.00(f) | | |
| muHgFA12 | 1.09(0.032) | 5.2(13)[e] | 0.00(1) | 1.00(f) | | |

[a] The numbers in parentheses indicate standard deviations of the last digits of the fitting parameters. f indicates parameter fixed during fitting. At pH 8.5 and 12, no FA layer structure was observed. [b] Descriptions of sample codes are given in the Experimental Section. [c] See Section SI4 of the Supporting Information for the definition. [d] Values are the averaged electron density of the layer normalized to that of bulk water over the unit cell area ($A_{UC}$). [e] Value is poorly determined because the occupancy of sorbed Hg was effectively nil.

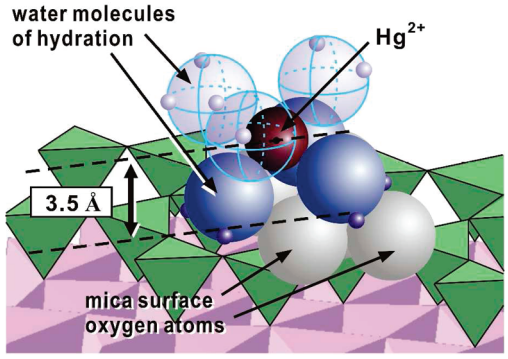


**FIGURE 4. One possible sorption geometry in which hydrated $Hg^{2+}$ approaches most closely to the basal surface of the muscovite mica. Three water molecules surrounding the central Hg(II) directly contact oxygen atoms of the muscovite surface: one is located in a ditrigonal cavity and the other two are above the triads of two adjacent $(SiO_4)^{4-}$ tetrahedra. See Section SI6 of the Supporting Information for other models.**

We can estimate a RCOOH:Hg(II) molar ratio of ~5:1 (i.e., 3.2 carboxylic groups versus 0.62(5) Hg(II) atom/$A_{UC}$) in the sorbed Hg(II)−FA species based on the total electron density and Hg concentration of the sorbed film, assuming there is no water in the FA film. In comparison, the molar ratio of RCOOH:Hg(II) in the muHgFA2 solution was much smaller (~1:1) based on the chemical composition of ESFA II (i.e., [RCOOH] = 13.24 mol $kg^{-1}C$ (*28*)) and concentration of $Hg(NO_3)_2$. There are two possibilities for the difference: (1) approximately three-fifths of the carboxylic groups of the film were inaccessible to $Hg^{2+}$, assuming adsorbed FA molecules have the same chemical composition as those remaining in solution and the $Hg^{2+}$−carboxyl group binding is bidentate, or (2) more hydrophobic FA molecules containing fewer acidic functional groups adsorbed preferentially on muscovite as observed for NOM sorption on clays (*29, 30*) and other minerals (*31*−*33*). If the film has the same ratio of carboxylic groups to Hg(II) as the initial solution, the only other way to explain this is by assuming that about 80% of the layer was composed of water, which was shown previously not to occur (*23*). These arguments support some type of conformational change in the adsorbed FA and/or partitioning of a different fraction of FA onto the muscovite surface.

**Reduced Uptake of Mercury(II) and Fulvic Acid with Increasing pH.** Mercury(II) uptake decreased by about 1 order of magnitude at pH 3.7 to 8.5 compared to that at pH 2 (Figure 5a). Total electron density profiles at pH 3.7 and 5.5, however, show film structures similar to those without Hg(II)

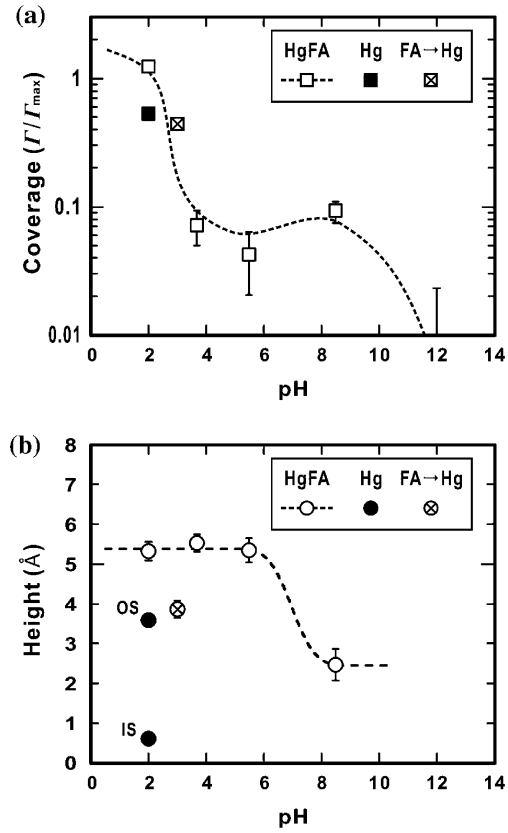


**FIGURE 5. Coverages [$\Gamma/\Gamma_{max}$, where $\Gamma$ is the amount of Hg determined from RAXR, and $\Gamma_{max}$ is the amount required to compensate the bare muscovite surface charge (0.966 $e^-/A_{UC}$) and average heights of Hg(II) sorbed onto the muscovite surface in 0.5−1 × $10^{-3}$ mol/kg $Hg(NO_3)_2$ and 100 mg/kg ESFA II solutions as a function of pH. The average height at pH 12 is not plotted because the occupancy of sorbed Hg was effectively nil (Table 1). Total occupancies and heights of inner-sphere (IS) and outer-sphere (OS) $Hg^{2+}$ in a 1 × $10^{-3}$ mol/kg $Hg(NO_3)_2$ solution at pH 2 (muHg2) and the total occupancy and average height in a solution of 100 mg/kg ESFA II to which 1 × $10^{-3}$ mol/kg $Hg(NO_3)_2$ was added (FAmuHg3) are also shown.**

at comparable pHs (Figure 3b and Figure S5a,b of the Supporting Information). The ratio of electron density of sorbed Hg to FA decreased [0.16→0.026→0.014, in terms of $W_{eq}(Hg)/W_{eq}(FA)$] as solution pH increased from 2 to 5.5, indicating that FA molecules with less Hg preferentially adsorbed onto the surface at higher pH. These results complement speculations that DOM can decrease metal uptake in systems with little or no solid NOM fractions by forming nonsorbing metal−organic complexes, including colloidal forms at acidic to basic pH (*9, 34*).

There is also a distinct change in the average height of the sorbed Hg(II) species from >5 Å at acidic to neutral pH to about 2.5 Å at alkaline pH (Figure 5b). The average height at lower pH is farther from the surface than the IS and OS species observed in muHg2 (without FA), indicating that sorbed Hg(II) must be in the form of an organic complex. This is consistent with thermodynamic calculations (Figure S1b of the Supporting Information) showing that dissolved Hg(II) occurs dominantly as Hg(II)−FA complexes up to pH of about 7. Above pH 7, the fraction of Hg(II)−FA solution complexes decreases, and the neutral inorganic species $Hg(OH)_2^0$ dominates according to thermodynamic calculations. The average height of 2.47(39) Å for Hg(II) at pH 8.5 suggests adsorption of this smaller inorganic species, which is compatible with the absence of a continuous FA film (*23*) (Figure S5c of the Supporting Information). Presumably, this Hg adsorbed as a partially or fully dehydroxylated Hg species on the negatively charged muscovite surface rather than the neutral $Hg(OH)_2^0$. At pH 12, there was no discernible adsorbed Hg [0.00(1) atom/$A_{UC}$], which may be attributed, in part, to competition with the highly concentrated $Na^+$ ions from NaOH added to adjust the pH.

**Mercury(II) Uptake in a Pre-existing Fulvic Acid Film.** Sorbed organic matter can increase uptake of metals on minerals significantly. For example, X-ray absorption near-edge structure (XANES) measurements showed that a larger fraction of Cu(II) adsorbed in HA coatings on goethite as the coverage of HA increased (*6*). Similar results were obtained for Pb(II) in biofilms on oxide minerals after the surface sites of the minerals were saturated at high solution concentrations of the metal ($10^{-6}$ to $10^{-3.5}$ M) using total external reflection X-ray standing wave (TER-XSW) measurements (*7*).

RAXR data show that Hg(II) was incorporated throughout a pre-existing FA film in an amount of 0.23(2) atom/$A_{UC}$ at pH 3 (Figure 3b). The broad distribution of Hg(II) is distinct from that of $Ba^{2+}$ at pH 3.7, where approximately 70% of the sorbed $Ba^{2+}$ penetrated the film and formed an IS species as it did in the absence of FA (*22*). The $Hg^{2+}$ may be trapped by the preadsorbed organic film before reaching its IS position at the muscovite surface because it is more organophilic than $Ba^{2+}$. For example, the 1:1 metal−ligand binding constant of $Hg^{2+}$ with carboxylic acid is $10^{5.55}$, much higher than the binding constant of $10^{0.14}$ for $Ba^{2+}$ (*35*). Furthermore, the $Hg^{2+}$ complexation in DOM has a large range of binding strengths from conditional constants on the order of $10^{10}$ for assumed monodentate complexation with carboxyl functional groups (*13, 36*) to values approximately 10 to 20 orders of magnitude higher for monodentate binding to thiol functional groups (*13, 14, 37, 38*).

Despite the interpretation that $Hg^{2+}$ is trapped in the film because of its large affinity for organic matter, we found the reflectivity data unexpectedly changed with time, in contrast to the stability of the reflectivity signal for uptake from premixed Hg(II)−FA solutions (Figure S4b of the Supporting Information). The greater X-ray beam sensitivity shows that binding of Hg(II) to the pre-existing FA film after 5 h of reaction is weaker than binding of Hg(II) to dissolved FA prior to uptake on the surface, which may mean that the adsorbed FA is either different in composition from that in the bulk solution or else underwent conformational changes that altered its binding behavior with the Hg cation. Evolution of the distribution of Hg(II) was monitored by measuring RAXR spectra at $q = 0.38$ Å$^{-1}$, and the amount and average height of Hg(II) were obtained using a model-independent analysis (*24*). The effective occupancy decreased from 0.23(2) to 0.11(2) atom/$A_{UC}$ after 2 h of exposure to X-ray radiation, indicating that either about 50% of the Hg(II) desorbed or the distribution width of the total Hg(II) profile increased substantially. However, the change in average position of Hg(II) was slight [from 3.9(1) to 3.7(2) Å], which implies that Hg(II) decreased evenly across the area of the FA film. The desorption might be linked to beam damage [e.g., photoreduction of the Hg(II) potentially aided by redox-sensitive moieties in the DOM and/or photolysis of water], but the lack of observed desorption under X-ray exposure of muscovite in contact with the premixed Hg−FA solutions indicates that the nature of Hg-binding to the preadsorbed film is different. To test if Hg(II) would readsorb, we turned off the X-ray beam for 30 min, after which RAXR spectra were remeasured on the same spot at the same *q*. The occupancy recovered partially to 0.17(2) atom/$A_{UC}$, indicating reversible uptake of Hg(II). The average height [4.4(3) Å] was, however, slightly larger than that prior to readsorption, implying slow diffusion of Hg(II) into the FA film.

**Utility of XR and RAXR for Probing Metal−Organic−Mineral Interactions.** The combination of XR and RAXR allows the distribution of Hg(II) within sorbed FA films to be observed in situ and with atomic-scale vertical resolution. By varying experimental conditions such as pH and the order in which muscovite was exposed to FA and Hg(II), we determined separate influences of the charged (001) surface, dissolved FA molecules, and preadsorbed FA film on Hg(II) uptake. This approach can be used to monitor and quantify metal adsorption at environmentally relevant mineral−water interfaces with a level of specificity and resolution that is necessary for understanding adsorption mechanisms in natural systems but is unobtainable by any other approach (e.g., compare to Grazing Incident EXAFS spectroscopy (*39−41*), which is element-specific but not interface-specific, and TER-XSW (*7*), which is element and interface specific but with a vertical resolution of >10 nanometers). In particular, the FA films have two roles: (1) they effectively block Hg(II) from binding directly to the muscovite surface as distinct IS and/or OS species and (2) provide binding sites within the ~1 nm thick organic layer but with a nontrivial relationship among vertical distribution, uptake amount, and cation binding strength. Although FA is only one type of organic matter that coats minerals in the environment, use of XR and RAXR together could be applied generally providing a new opportunity to develop accurate physical models that incorporate competitive adsorption, diffusion, solution speciation, and other chemical reactions at mineral−water interfaces relevant to the fate and transport of toxic metals.

## Acknowledgments

This work was funded by the Geosciences Research Program, Office of Basic Energy Sciences, U.S. Department of Energy (DOE) under Grant DE-FG02-06ER15364 to the University of Illinois at Chicago (UIC) and Contract DE-AC02-06CH11357 to UChicago Argonne LLC as operator of Argonne National Laboratory and by the Geobiology and Low-Temperature Geochemistry Program of the National Science Foundation under Grant EAR-0447310 to UIC. Use of the APS was supported by the DOE, Office of Basic Energy Sciences.

## Supporting Information Available

Mercury(II) speciation calculations, details of the XR measurements and analyses, resonant dispersion of $Hg^{2+}$, and electron density profiles at pH 3.7−12. This material is available free of charge via the Internet at http://pubs.acs.org.

## Literature Cited


(1) Benoit, J. M.; Gilmour, C. C.; Mason, R. P.; Riedel, G. S.; Riedel, G. F. Behavior of mercury in the Patuxent River estuary. *Biogeochem.* **1998**, *40*, 249–265.

(2) Choe, K.-Y.; Gill, G. A.; Lehman, R. Distribution of particulate, colloidal, and dissolved mercury in San Francisco Bay estuary. 1. Total mercury. *Limnol. Oceanogr.* **2003**, *48*, 1535–1546.

(3) Slowey, A.; Johnson, S. B.; Rytuba, J. J.; Brown, G. E., Jr. Role of organic acids in promoting colloidal transport of mercury from mine tailings. *Environ. Sci. Technol.* **2005**, *39*, 7869–7874.

(4) Hammerschmidt, C. R.; Fitzgerald, W. F. Geochemical controls on the production and distribution of methylmercury in near-shore marine sediments. *Environ. Sci. Technol.* **2004**, *38*, 1487–1495.

(5) Drott, A.; Lambertsson, L.; Björn, E.; Skyllberg, U. Importance of dissolved neutral mercury sulfides for methyl mercury production in contaminated sediments. *Environ. Sci. Technol.* **2007**, *41*, 2270–2276.

(6) Alcacio, T. E.; Hesterberg, D.; Chou, J. W.; Martin, J. D.; Beauchemin, S.; Sayers, D. E. Molecular scale characteristics of Cu(II) bonding in goethite-humate complexes. *Geochim. Cosmochim. Acta* **2001**, *65* (9), 1355–1366.

(7) Templeton, A. S.; Trainor, T. P.; Traina, S. J.; Spormann, A. M.; Brown, G. E., Jr. Pb(II) distributions at biofilm−metal oxide interfaces. *Proc. Natl. Acad. Sci.* **2001**, *98*, 11897–11902.

(8) Bäckström, M.; Dario, M.; Karlsson, S.; Allard, B. Effects of a fulvic acid on the adsorption of mercury and cadmium on goethite. *Sci. Total Environ.* **2003**, *304*, 257–268.

(9) Arias, M.; Barral, M. T.; Da Silva-Carvalhal, J.; Mejuto, J. C.; Rubinos, D. Interaction of Hg(II) with kaolin−humic acid complexes. *Clay Miner.* **2004**, *39*, 35–45.

(10) Xia, K.; Skyllberg, U. L.; Bleam, W. F.; Bloom, P. R.; Nater, E. A.; Helmke, P. A. X-ray absorption spectroscopic evidence for the complexation of Hg(II) by reduced sulfur in soil humic substances. *Environ. Sci. Technol.* **1999**, *33*, 257–261.

(11) Hesterberg, D.; Chou, J. W.; Hutchison, K. J.; Sayers, D. E. Bonding of Hg(II) to reduced organic sulfur in humic acid as affected by S/Hg ratio. *Environ. Sci. Technol.* **2001**, *35*, 2741–2745.

(12) Drexel, R. T.; Haitzer, M.; Ryan, J. N.; Aiken, G. R.; Nagy, K. L. Mercury(II) sorption to two Florida Everglades peats: Evidence for strong and weak binding and competition by dissolved organic matter released from the peat. *Environ. Sci. Technol.* **2002**, *36*, 4058–4064.

(13) Haitzer, M.; Aiken, G. R.; Ryan, J. N. Binding of mercury(II) to dissolved organic matter: The role of the mercury-to-DOM concentration ratio. *Environ. Sci. Technol.* **2002**, *36*, 3564–3570.

(14) Khwaja, A. R.; Bloom, P. R.; Brezonik, P. L. Binding constants of divalent mercury ($Hg^{2+}$) in soil humic acids and soil organic matter. *Environ. Sci. Technol.* **2006**, *40*, 844–849.

(15) Skyllberg, U.; Bloom, P. R.; Qian, J.; Lin, C.-M.; Bleam, W. F. Complexation of mercury(II) in soil organic matter: EXAFS evidence for linear two-coordination with reduced sulfur groups. *Environ. Sci. Technol.* **2006**, *40*, 4174–4180.

(16) Fenter, P.; Sturchio, N. C. Structure and growth of stearate monolayers on calcite: First results of an in situ X-ray reflectivity study. *Geochim. Cosmochim. Acta* **1999**, *63*, 3145–3152.

(17) Cheng, L.; Fenter, P.; Nagy, K. L.; Schlegel, M. L.; Sturchio, N. C. Molecular-scale density oscillations in water adjacent to a mica surface. *Phys. Rev. Lett.* **2001**, *87*, 1561031−4.

(18) Fenter, P. A. X-ray Reflectivity as a Probe of Mineral−Fluid Interfaces: A user guide. In *Application of Synchrotron Radiation in Low-Temperature Geochemistry and Environmental Science, Reviews in Mineralogy and Geochemistry*; Fenter, P. A., Rivers, M. L., Sturchio, N. C., Sutton, S. R., Eds.; Geochemical Society and Mineralogical Society of America: Washington, DC, 2002; Vol. 49, pp 149−220.

(19) Schlegel, M. L.; Nagy, K. L.; Fenter, P.; Cheng, L.; Sturchio, N. C.; Jacobsen, S. D. Cation sorption on the muscovite (001) surface in chloride solutions using high-resolution X-ray reflectivity. *Geochim. Cosmochim. Acta* **2006**, *70*, 3549–3565.

(20) Park, C.; Fenter, P. A.; Nagy, K. L.; Sturchio, N. C. Hydration and distribution of ions at the mica−water interface. *Phys. Rev. Lett.* **2006**, *97*, 016101−1-4.

(21) Park, C.; Fenter, P. A.; Sturchio, N. C.; Nagy, K. L. Thermodynamics, interfacial structure, and pH hysteresis of $Rb^{+}$ and $Sr^{2+}$ adsorption at the muscovite (001)−solution interface. *Langmuir* **2008**, *24*, 13993–14004.

(22) Lee, S. S.; Nagy, K. L.; Fenter, P. Distribution of barium and fulvic acid at the mica−solution interface using in-situ X-ray reflectivity. *Geochim. Cosmochim. Acta* **2007**, *71*, 5763–5781.

(23) Lee, S. S.; Fenter, P.; Park, C.; Nagy, K. L. Fulvic acid sorption on muscovite mica as a function of pH and time using in situ X-ray reflectivity. *Langmuir* **2008**, *24*, 7817–7829.

(24) Park, C.; Fenter, P. A. Phasing of resonant anomalous X-ray reflectivity spectra and direct Fourier synthesis of element-specific partial structures at buried interfaces. *J. Appl. Crystallogr.* **2007**, *40*, 290–301.

(25) Richens, D. T. *The Chemistry of Aqua Ions*. John Wiley & Sons, Ltd.: West Sussex, England, 1997; p 592.

(26) Hiemenz, P. C.; Rajagopalan, R. *Principles of Colloid and Surface Chemistry*, 3rd ed.; Marcel Dekker, Inc.: New York, 1997.

(27) Brigatti, M. F.; Colonna, S.; Malferrari, D.; Medici, L.; Poppi, L. Mercury adsorption by montmorillonite and vermiculite: A combined XRD, TG-MS, and EXAFS study. *Appl. Clay Sci.* **2005**, *28*, 1–8.

(28) Ritchie, J. D.; Perdue, E. M. Proton-binding study of standard and reference fulvic acids, humic acids, and natural organic matter. *Geochim. Cosmochim. Acta* **2003**, *67* (1), 85–96.

(29) Feng, X.; Simpson, A. J.; Simpson, M. J. Chemical and mineralogical controls on humic acid sorption to clay mineral surfaces. *Org. Geochem.* **2005**, *36*, 1553–1566.

(30) Simpson, A. J.; Simpson, M. J.; Kingery, W. L.; Lefebvre, B. A.; Moser, A.; Williams, A. J.; Kvasha, M.; Kelleher, B. P. The application of 1H high-resolution magic-angle spinning NMR for the study of clay−organic associations in natural and synthetic complexes. *Langmuir* **2006**, *22*, 4498–4503.

(31) Ochs, M.; Ćosćović, B.; Stumm, W. Coordinative and hydrophobic interaction of humic substances with hydrophilic $Al_2O_3$ and hydrophobic mercury surfaces. *Geochim. Cosmochim. Acta* **1994**, *58*, 639–650.

(32) Meier, M.; Namjesnik-Dejanovic, K.; Maurice, P. A.; Chin, Y.-P.; Aiken, G. R. Fractionation of aquatic natural organic matter upon sorption to goethite and kaolinite. *Chem. Geol.* **1999**, *157*, 275–284.

(33) Hur, J.; Schlautman, M. A. Molecular weight fractionation of humic substances by adsorption onto minerals. *J. Colloid Interface Sci.* **2003**, *264*, 313–321.

(34) Boily, J.-F.; Fein, J. B. Proton binding to humic acids and sorption of Pb(II) and humic acid to the corundum surface. *Chem. Geol.* **2000**, *168*, 239–253.

(35) Martell, A. F.; Smith, R. M. *Critical Stability Constants: Other Organic Ligands*: Plenum Press: New York, 1976; Vol. 3H, p 495.

(36) Lövgren, L.; Sjöberg, S. Equilibrium approaches to natural water systems 7. Complexation reactions of copper(II), cadmium(II) and mercury(II) with dissolved organic matter in a concentrated bog water. *Water Res.* **1989**, *23*, 327–332.

(37) Haitzer, M.; Aiken, G. R.; Ryan, J. N. Binding of mercury (II) to aquatic humic substances: Influence of pH and source of humic substances. *Environ. Sci. Technol.* **2003**, *37*, 2436–2441.

(38) Skyllberg, U. Competition among thiols and inorganic sulfides and polysulfides for Hg and MeHg in wetland soils and sediments under suboxic conditions: Illumination of controversies and implications for MeHg net production. *J. Geophys. Res.* **2008**, *113*, G00C03−1-14.

(39) Den Auwer, C.; Drot, R.; Simoni, E.; Conradson, S. D.; Gailhanou, M.; de Leon, J. M. Grazing incidence XAFS spectroscopy of uranyl sorbed onto $TiO_2$ rutile surfaces. *New J. Chem.* **2003**, *27*, 648–655.

(40) Denecke, M. A.; Dardenne, R. K.; Lindqvist-Reis, P. Grazing incidence (GI) XAFS measurements of Hf(IV) and U(VI) sorption onto mineral surfaces. *Phys. Chem. Chem. Phys.* **2003**, *5*, 939–946.

(41) Bargar, J. R.; Trainer, T. P.; Fitts, J. P.; Chambers, S. A.; Brown, G. E., Jr. In situ grazing-incidence extended X-ray absorption fine structure study of Pb(II) chemisorption on hematite (0001) and (1−102) surfaces. *Langmuir* **2004**, *20*, 1667–1673.


ES900214E